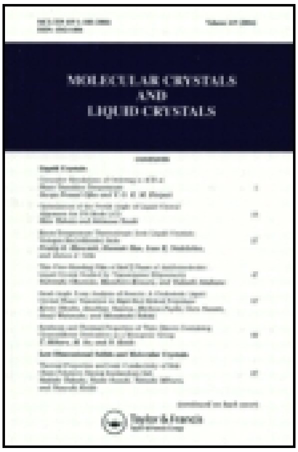

Molecular Crystals and Liquid Crystals
Publication details, including instructions for authors and subscription information:
http://www.tandfonline.com/loi/gmcl20

Infiltration of E7 Liquid Crystal in a Nanoparticle-Based Multilayer Photonic Crystal: Fabrication and Electro-optical Characterization

Luigino Criante [a] & Francesco Scotognella [b]

[a] Center for Nano Science and Technology @ PoliMi , Istituto Italiano di Tecnologia , Pascoli , Milano

[b] Dipartimento di Fisica , Istituto di Fotonica e Nanotecnologie CNR, Politecnico di Milano , Milano , Italy

Published online: 02 Apr 2013.

Mol. Cryst. Liq. Cryst., Vol. 572: pp. 31–39, 2013

ISSN: 1542-1406 print/1563-5287 online
DOI: 10.1080/15421406.2012.763207

Infiltration of E7 Liquid Crystal in a Nanoparticle-Based Multilayer Photonic Crystal: Fabrication and Electro-optical Characterization

LUIGINO CRIANTE[1,*] AND FRANCESCO SCOTOGNELLA[2]

[1]Center for Nano Science and Technology @ PoliMi, Istituto Italiano di Tecnologia, Pascoli, Milano
[2]Dipartimento di Fisica, Istituto di Fotonica e Nanotecnologie CNR, Politecnico di Milano, Milano, Italy

In this study, we propose the fabrication and the electro-optical characterization of nanoparticle-based multilayer photonic crystals infiltrated with a nematic liquid crystal. Two methods of the photonics band gap tunability have been proposed. In the first, we have observed an aligning of the liquid crystal director along the external electric field vector at very low applied voltage, with a blue shift of the photonic band gap of 8 nm at only 8 V_{rms}. *In the second, we put forward the possibility of tuning the photonic band gap of the porous multilayer just by infiltration of appropriate liquid crystals, in accordance with results carried out by a custom simulation software. The presented device could be very interesting for applications where high sensitivity sensor and selective color tunability is needed with the use of cheap and low-voltage power supplies.*

Keywords Photonic crystals; liquid crystals; nano-particles; electric field; infiltration; color tenability

Introduction

Materials with intermixed phases of different materials at a nanometer level could show interesting characteristics due to a superimposition of the constituting compounds properties, giving rise to new unique properties. In the field of materials science, several methods have been developed to obtain these types of nanomaterials [1]. A very successful example is the bulk heterojunction in organic photovoltaics, where two polymers are deposited starting from the same solution (usually by spin coating) in order to obtain a blend where nanometric domains allow an efficient exciton diffusion to the polymer/polymer interface, where exciton dissociation occurs [2–6]. Another example is the dye-sensitized solar cell, where a monolayer of organic dye binds the surface of a porous layer made of metal oxide nanoparticles. In such a cell, an efficient electron transport occurs from the dye (excited by the sun) to the nanoparticle [7–11].

The number of research groups that are studying the infiltration of porous layers made of nanoparticles has increased owing to the easy fabrication of nanoparticle layers and the facile and cheap infiltration of such layers with different kinds of materials [12–14].

*Address correspondence to Luigino Criante, Center for Nano Science and Technology @ PoliMi, Istituto Italiano di Tecnologia, Via Giovanni Pascoli, 70/3, 20133 Milano. Tel.: +39 02 23996056; Fax: +39 02 23999866. E-mail: luigino.criante@iit.it

Among the diverse typologies of porous layered materials, a very interesting class is the multilayer photonic crystal [15]. Multilayer photonic crystals are a type of one-dimensional photonic crystals in which the periodic alternation of layers made by two different materials results in an ordered modulation of the dielectric constant, with a periodicity close to the wavelength. In these materials, according to the Bragg–Snell law, a narrow range of wavelengths of the electromagnetic radiation are reflected back, while the other wavelengths are transmitted [15–19].

The porous multilayer shows pores between the constituting nanoparticles, which in principle can be infiltrated by any compound. With the infiltration of materials possessing optical gain, it is possible to make distributed feedback laser by one-photon [20–22] and two-photon pumping [23]. If the porous photonic crystal, coupled with a TiO_2 electrode, is infiltrated with a dye, an efficient dye-sensitized solar cell is obtained [24]. A catchy technique is the infiltration of liquid crystals in photonic structure that allows the tuning of the photonic properties by taking advantages of the response of liquid crystals to external stimuli, such as temperature or electric field. While synthetic opals and random photonic structures infiltrated with liquid crystals are widely described in the literature [25–27], only recently, the infiltration of liquid crystals in photonic multilayers has been reported [28]. In these novel devices, it is easy to obtain very high refractive index modulations by only alternating two or more suitable nanoparticle materials. An interesting consequence is the capability to achieve significant photonic band gap efficiency with a thickness of just few micrometers. In fact, the photonic band gap efficiency is proportional to $\Delta n \cdot d$, where Δn is the amplitude modulation of the refractive index and d is the thickness of the sample. To increase the thickness would be detrimental, since the electrical tuning will require a large applied electric voltage [27,29]. Therefore, in order to take advantage of both, a low-voltage tuning and good band gap efficiency, the photonics multilayers based on nanoparticle could be the best strategy to obtain a high refractive index contrast (Δn) and to arrange a small-thickness device.

Here, we present the fabrication of a porous multilayer photonic crystal and its infiltration with the E7 liquid crystal. We have studied the optical properties of this nanocomposite material by employing the transfer matrix method (TMM) as a theoretical analysis, and we have shown the possibility to tune its optical properties by applying very low electric voltage. Furthermore, an alternative technique to easily tune the photonic crystal proprieties has been proposed.

Experimental Section

We have used colloidal dispersions of silicon dioxide and zirconium dioxide to realize the multilayer photonic crystal. Silicon dioxide and zirconium dioxide colloidal dispersions are purchased from Alfa Aesar. Silicon (zirconium) dioxide nanoparticles have an average size of 100 nm and are dispersed in ethylene glycol (water) with a concentration of 30% (10%) in weight. The E7 liquid crystal mixture, composed by 4-cyano-4-*n*-pentyl-biphenyl (5CB), 4-cyano-4-nheptylbiphenyl (7CB), 4-cyano-4-*n*-octyloxy-biphenyl, and 4-cyano-4-*n*-pentyl-*p*-terphenyl, was purchased from the Merck Liquid Crystal. In the visible range (from 400 to 650 nm) and at room temperature, the extraordinary refractive index (n_e) increases from 1.73 to 1.80, while its ordinary refractive index (n_o) also increases slowly from 1.52 to 1.54 [30]. Its isotropic refractive indexes (at 589 nm) n_{iso} is $\approx$1.575, while in the near-infrared region, Δn is about 0.186 at 1.55 μm [31].

The photonic multilayer has been deposited by spin coating technique. The sample substrate is indium tin oxide (ITO) glass, previously sonicated for 10 minutes in acetone and

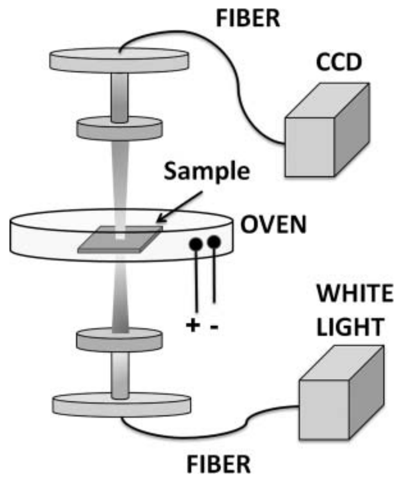

Figure 1. Scheme of the setup for light transmission measurements. Light from a tungsten lamp is collimated on the sample. Transmitted light is then detected by a concave grating spectrometer. The sample is placed in an oven with electrical contacts to apply electric field on the sample.

isopropanol. The spin coater is a Laurell WS-400–6NPP-Lite, and the speeds of rotation were 6000 and 3000 rpm for silicon dioxide and zirconium dioxide, respectively (with a rotation time of 30 seconds). After each layer deposition, the sample was heated at a temperature of 350°C for 20 minutes in air.

Morphological characterization of the samples (before infiltration) has been performed by Alpha Step profilometer and JEOL scanning electron microscope (SEM). The optical characterization has been performed by using a tungsten lamp and a concave grating spectrometer from Stellarnet (spectral resolution 1.5 nm). Infiltration has been done with electronically controlled Teflon oven (CaLCTech), and monitored in real time with the optical equipment reported in Fig. 1.

A deep study of the optical properties of the multilayer, taking into account the dispersion of all used materials, has been carry out using the TMM. We have considered the system air/multilayer/glass (in which glass is the substrate), with the light coming out in the glass substrate. n_0 and n_s are the refractive indexes of air and glass, respectively, while E_m and H_m are the electric and magnetic fields in the glass substrate. To determine the electric and magnetic fields in air, E_0 and H_0, we have solved the following system:

$$\begin{bmatrix} E_0 \\ H_0 \end{bmatrix} = M_1 \cdot M_2 \cdot ..... \cdot M_m \begin{bmatrix} E_m \\ H_m \end{bmatrix}, \quad (1)$$

where

$$M_j = \begin{bmatrix} \cos\phi_j & \frac{i \cdot \sin\phi_j}{n_j} \\ i \cdot n_j \cdot \sin\phi_j & \cos\phi_j \end{bmatrix}, j = 1, \ \ldots, \ m, \quad (2)$$

and $\phi_j = k \cdot n_j \cdot d_j$, that is, the phase variation of the wave passing the layer j, with k being the wavenumber depending on the wavelength of the incident light by $k = 2\pi/\lambda$. Inserting Equation (2) into Equation (1) and using the definition of transmission coefficient, it is

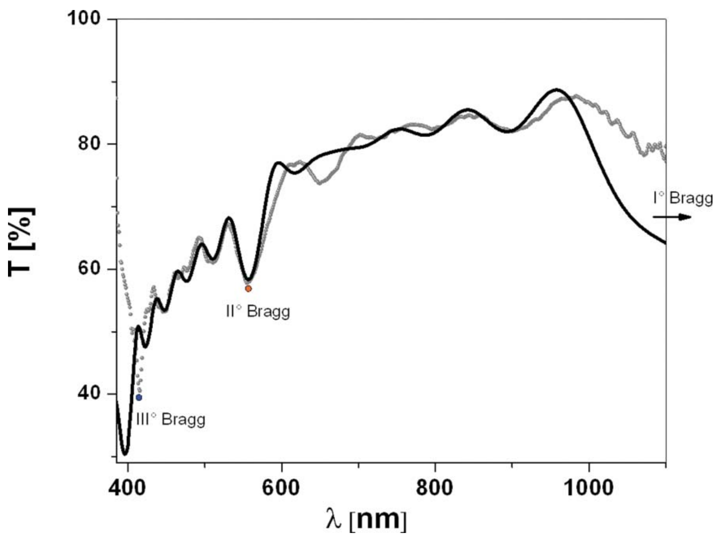

Figure 2. Experimental (light gray filled circle) and simulation (by the transfer matrix method, black line) transmission spectrum of six bilayer photonic crystal made of alternated zirconium dioxide and silicon dioxide nanoparticles. The fundamental, the second, and third order of the photonic band gap are indicated in the plot. The simulation takes into account the dispersion of the materials and the losses due to light scattering.

possible to write the light transmission as

$$T = \frac{4n_s}{n_0 \left| E_0 + \frac{H_0}{n_0} \right|^2}. \quad (3)$$

Results and Discussion

In Fig. 2, the transmission spectrum of the fabricated multilayer photonic crystal is reported (light gray filled circle). The first-order photonic band gap arises around 1100 nm (at the border of the detectable spectral window by the experimental apparatus), a second order at 565 nm, and a third order at 410 nm, according to the Bragg–Snell law for this structure.

As a matter of fact, it is possible to characterize a multilayer photonic crystal in accordance with the Bragg regime (or two-wave regime) diffraction only if a *thick* grating (or *volume* grating) has been obtained. The following are the two conditions that should be fulfilled:

$$Q = K^2 \lambda d/(2\pi n_m) > 1 \quad \text{and} \quad \rho = \lambda^2/(\Lambda n_m \Delta n) \geq 10,$$

where $K = 2\pi/\Lambda$ is a grating vector, Λ is the grating spacing, d is the sample thickness, n_m is the average refractive index, Δn is the index modulation for the dielectric grating, and λ is the vacuum wavelength spacing [32]. Despite the small sample thickness of our sample (six bilayers), the two above conditions are fulfilled, beginning already in the visible range. Besides, we point out that the peak positions of the Bragg diffraction high orders are strictly affected by the dispersion of the materials, especially at high frequency.

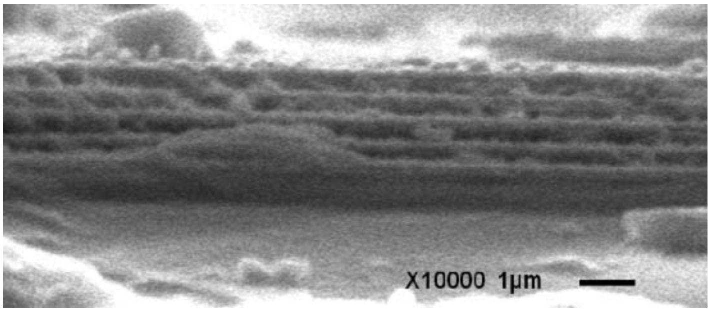

Figure 3. SEM cross-section image of the six bilayer nanoparticle photonic crystal (magnification 10,000×, scale bar: 1 μm).

The thicknesses of the layers can be extracted from profilometry measurements and confirmed by the SEM cross-section image (see Fig. 3). The sum of the thicknesses of the SiO_2 (light gray in the SEM image) and the ZrO_2 layer (dark gray in the SEM image) results in a unit cell thickness of $\Lambda = 380$ nm (Λ is the pitch of the photonic crystal) such that the overall multilayer thickness, which is six bilayers, is around 2300 nm. We attributed the decrease in experimental transmission, at shorter wavelengths, mainly to a significant scattering of light due to the relatively large size of the nanoparticles in the zirconium dioxide layer (100 nm).

For a better understanding, the optical properties of the photonic structure, a simulation of the spectrum by the TMM is reported (Fig. 2, black line). For the silicon dioxide refractive index dispersion, we have used the Sellmeier equation reported in Ref. [33], while for the zirconium dioxide, we have used tabulated data from the website: refractiveindex.info. For the liquid crystal E7, the Cauchy equation that usually described the dispersion relationship between refractive index and wavelength has been taken from Li et al. [30]. The simulation is in good agreement with the experimental data, testified by matching of the three orders of the Bragg peak wavelength position with the simulated ones. The scattering losses in the simulation model have been considered by using a Rayleigh scattering curve. We also take into account the constant loss due to the ITO-coated glass support (5% over all the spectral region). Further theoretical studies will be devoted to the losses in such photonic systems. In the simulations, we use as parameters the layers thicknesses and their porosity. The calculated thicknesses fit well with the SEM image, whereas we can tentatively conclude that the porosity of the SiO2 nanoparticle layer is about 25% and the porosity of the ZrO2 nanoparticle layer is about 50%.

Figure 4(a) shows the transmission spectra of the photonic structure before (gray dashed dot line) and after (black solid line) the infiltration process. The third order of the photonic band gap is indicated. To allow an efficient infiltration of the photonic crystal, we reached the temperature corresponding to the isotropic phase transition of the liquid crystal. After the infiltration, returning at room temperature and considering the pitch Λ of the photonic structure, the final wavelength position of the photonic band gap is strictly connected to the refractive index of the used materials (especially to that of liquid crystal defined as $(2n_o+n_e)/3$, for a random orientation of the liquid crystal directors, due to the irregular shapes of pores in the nanoparticle multilayer). In our case, the third order of the photonics band gap shows a shift toward longer wavelengths of about 50 nm. We underline that such third-order band gap wavelength position is in agreement with our theoretical

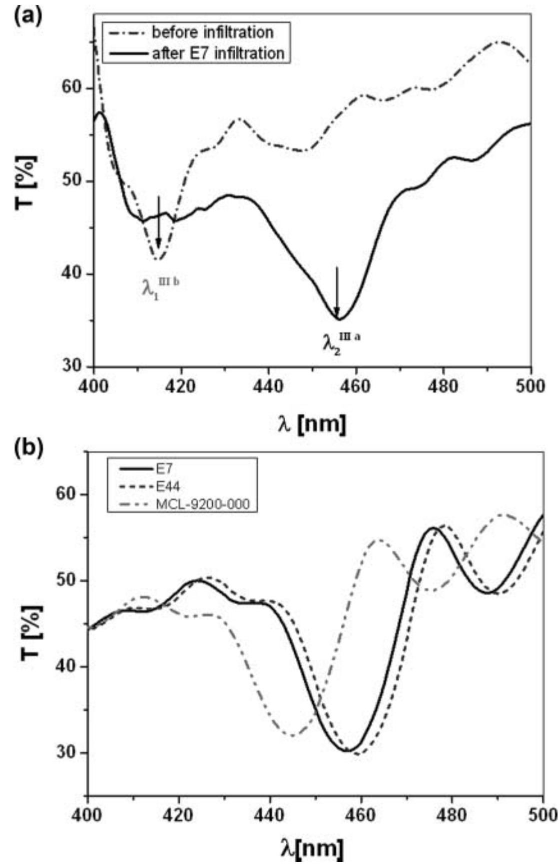

Figure 4. (a) Experimental transmission spectrum of the third Bragg order of six bilayer photonic crystal before (gray dashed dot line) and after (black solid line) E7 liquid crystal infiltration. (b) Simulation of transmission spectra of the third-order photonic band gap of the photonic crystal infiltrated with three different liquid crystals.

prevision, taking into account the value of the liquid crystal refractive index defined for a random orientation, as shown in Fig. 4(b) (black line).

By using the same geometrical and optical parameters of the aforementioned porous photonic structure and by using the TMM, it is possible to predict the light transmission properties of such structure infiltrated with different liquid crystals. In Fig. 4(b), we report the third-order photonic band gap of the structure infiltrated with E7, E44, and MLC9200–000 liquid crystals, which are commonly used for photonic applications. The optical properties of these liquid crystals have been taken from the website: refractiveindex.info. We observe that the shift due to infiltration is different for each liquid crystal, envisaging the possibility to select a particular wavelength just by choosing the proper material.

In order to tune the position of the photonic band gap with the electric field, we have prepared a device as depicted in Fig. 5(a). An additional ITO-coated glass has been superimposed on the sample and electrical contacts are applied. An estimation of the electrode distance is very difficult for our sample; thus, we have considered it as minimum

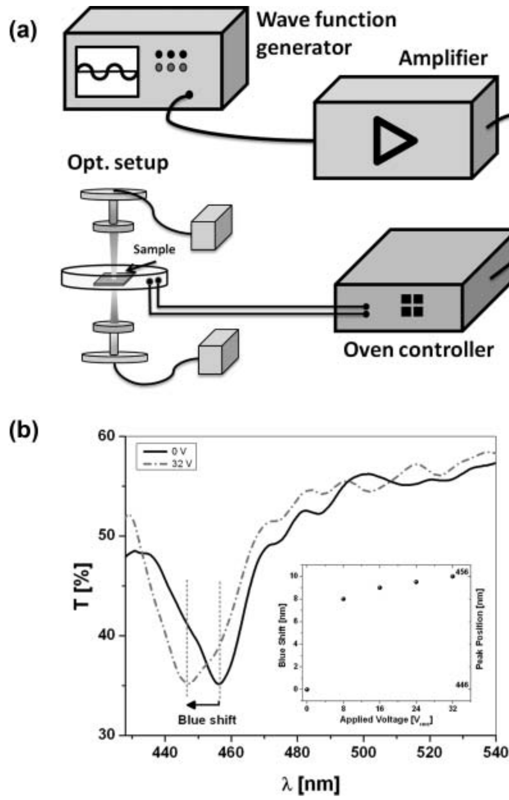

Figure 5. (a) Scheme of the experimental setup for photonic band gap tuning by applying the electric field. (b) Blue shift of the third-order photonic band gap by applying the electric field. Inset: Spectral position of the third-order photonic band gap center as a function of the electric voltage.

as possible, that is, the photonic crystal thickness that is 2.3 μm, even if such electrode distance is reasonably larger due to a nonperfect adhesion of the additional ITO electrode on the infiltrated photonic crystal. Applying an external voltage on the device (sine wave at 1 kHz), we observed a blue shift of the photonic band gap position (Fig. 5(b)).

It is noteworthy that we could get a significant shift of 8 nm with a very low voltage, that is, 8 V (rms), taking advantage from the very thin thickness of the device. The corresponding applied electric field is about 3.4 V/μm, one order of magnitude smaller with respect to what has been reported for similar devices [27,34] and lower (about 30%) with respect to the best performance by the porous silicon [29]. A further blue shift has been observed by increasing the applied voltage reaching saturation at 10 nm, that is, tuning from 446 to 456 nm.

Conclusions

In this work, we present the fabrication and characterization of a porous multilayer photonic crystals and its infiltration with the E7 liquid crystal. The infiltration results in a red shift of about 50 nm in the photonic band gap position, but it is possible to select a particular wavelength just by choosing the proper material. The photonic properties of the structure are in agreement with the theoretical analysis by the TMM. Applying an external electric voltage of 32 V (rms) to the multilayer, we observe a blue shift of 10 nm of the third-order Bragg peak. However, it is noteworthy that a shift of 8 nm (the larger shift increase) is already observable at very low electric voltage (8 V, rms). Furthermore, we propose the possibility to tune the photonic band gap of the porous multilayer just by infiltration of different liquid crystals, which is an easy alternative method to the fabrication of photonic crystals with different lattice parameters. The presented device could be very interesting for applications where high sensitivity sensor and/or selective color tunability is necessary with the employment of cheap and low-voltage power supplies.

Acknowledgments

The authors thank Prof. Francesco Simoni and Prof. Guglielmo Lanzani for support and helpful discussions. The authors acknowledge the Optical Laboratory at SIMAU Department (Università Politecnica delle Marche, Ancona, Italy) for technical support and the project FP7-ICT-248052 (PHOTOFET) for financial support.

References

[1] Ajayan, P. M., Schadler, L. S., & Braun, P. V. (2003). *Nanocomposite Science and Technology*, Wiley-VCH Verlag: Berlin.
[2] Li, G., Shrotriya, V., Huang, J., Yao, Y., Moriarty, T., Emery, K., & Yang, Y. (2005). *Nat. Mater.*, *4*, 864.
[3] Ma, W. L., Yang, C. Y., Gong, X., Lee, K., & Heeger, A. J. (2005). *Adv. Func. Mater.*, *15*, 1617.
[4] Holgesen, M., Sondergaard, R., & Krebs, F. C. (2010). *J. Mater. Chem.*, *20*, 36.
[5] Clarke, T. M., & Durrant, J. R. (2010). *Chem. Rev.*, *110*, 6736.
[6] Li, Y. F. (2010). *Acc. Chem. Rev.*, *45*, 723.
[7] ORegan, B., & Gratzel, M. (1991). *Nature*, *353*, 737.
[8] Gratzel, M. (2001). *Nature*, *414*, 338.
[9] Mor, G. K., Shankar, K., Paulose, M., Varghese, O. K., & Grimes, C. A. (2006). *Nano Lett.*, *6*, 215.
[10] Snaith, H. J., & Schmidt-Mende, L. (2007). *Adv. Mater.*, *19*, 3187.
[11] Kim, M. R., Jin, S. H., Park, S. H., Lee, H. J., Kang, E. H., & Lee, J. K. (2006). *Mol. Cryst. Liq. Cryst.*, *444*, 233.
[12] McLeary, E. E., Jansen, J. C., & Kapteijn, F. (2006). *Micropor. Mesopor. Mat.*, *90*, 198.
[13] Redel, E., Mirtchev, P., Huai, C., Petrov, S., & Ozin, G. A. (2011). *ACS Nano*, *5*, 2861.
[14] Puzzo, D. P., Bonifacio, L. D., Oreopoulos, J., Yip, C. M., Manners, I., & Ozin, G. A. (2009). *J. Mater. Chem.*, *19*, 3500.
[15] Joannopoulos, J. D., Meade, R. D., & Winn, J. N. (1995). *Photonic Crystals: Molding the Flow of Light*, Princeton University Press: Princeton, NJ.
[16] Scotognella, F., Monguzzi, A., Meinardi, F., & Tubino, R. (2010). *Phys. Chem. Chem. Phys.*, *12*, 337.
[17] Fink, Y., Winn, J. N., Fan, S. H., Chen, C. P., Michel, J., Joannopoulos, J. D., & Thomas, E. L. (1998). *Science*, *282*, 1679.
[18] Komikado, T., Yoshida, S., & Umegaki, S. (2006). *Appl. Phys. Lett.*, *89*, 061123.
[19] Frezza, L., Patrini, M., Liscidini, M., & Comoretto, D. (2011). *J. Phys. Chem. C*, *115*, 19939.
[20] Scotognella, F., Puzzo, D. P., Monguzzi, A., Wiersma, D. S., Maschke, D., Tubino, R., & Ozin, G. A. (2009). *Small*, *5*, 2048.
[21] Puzzo, D. P., Scotognella, F., Zavelani-Rossi, M., Sebastian, M., Lough, A. J., Manners, I., Lanzani, G., Tubino, R., & Ozin, G. A. (2009). *Nano Lett.*, *9*, 4273.
[22] Criante, L., Lucchetta, D. E., Vita, F., Castagna, R., & Simoni, F. (2009). *Appl. Phys. Lett.*, *94*, 111114.

[23] Scotognella, F., Puzzo, D. P., Zavelani-Rossi, M., Clark, J., Sebastian, M., Ozin, G. A., & Lanzani, G. (2011). *Chem. Mater.*, *23*, 805.
[24] Colodrero, S., Forneli, A., Lopez-Lopez, C., Pellejà, L., Miguez, H., & Palamares, E. (2012). *Adv. Func. Mater.*, *22*, 1303.
[25] Yoshino, K. Shimoda, Y., Kawagishi, Y., Nakayama, K., & Ozaki, M. (1999). *M. Appl. Phys. Lett.*, *75*, 932.
[26] Gottardo, S., Cavalieri, S., Yaroshchuk, O., & Wiersma, D. S. (2004). *Phys. Rev. Lett.*, *93*, 263901.
[27] Gottardo, S., Wiersma, D. S., & Vos, W. L. (2003). *Physica B*, *338*, 143.
[28] Criante, L., & Scotognella, F. (2012). *J. Phys. Chem. C*, *116*, 21572.
[29] Tkachenko, V., Dyomin, A. A., Tkachenko, G. V., Abbate, G., & Sukhoivanov, I. A. (2008). *J. Opt. A: Pure Appl. Opt.*, *10*, 055301.
[30] Li, J., Wench, C.-H., Gauza, S., Lu, R., & Wu, S.-T. (2005). *J. Disp. Technol.*, *1*, 51.
[31] Li, J., Wu, S.-T., Brugioni, S., Meucci, R., & Faetti, S. (2005). *J. Appl. Phys.*, *97*, 073501.
[32] Gaylord, T. K., & Moharam, M. G. (1981). *Appl. Opt.*, *20*, 3271–3273.
[33] Ghosh, G. (1999). *Opt. Comm.*, *163*, 95.
[34] Escuti, M. J., Qi, J., & Crawford, G. P. (2003). *Appl. Phys. Lett.*, *83*, 1331.